

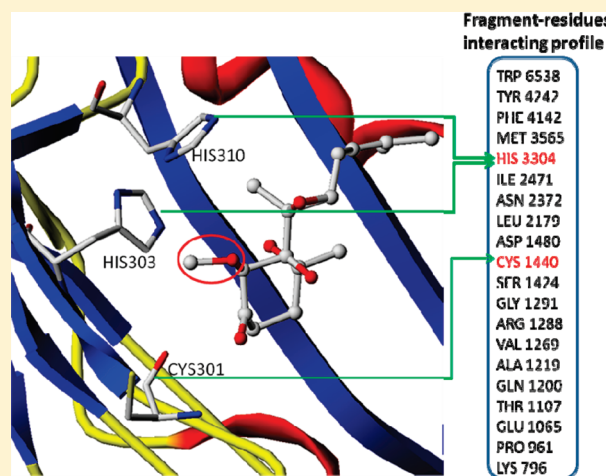
Residue Preference Mapping of Ligand Fragments in the Protein Data Bank

Lirong Wang,^{†,‡,§} Zhaojun Xie,[†] Peter Wipf,^{†,‡,§} and Xiang-Qun Xie^{*,†,‡,§,⊥}

[†]Department of Pharmaceutical Sciences, School of Pharmacy, [‡]Center for Chemical Methodologies & Library Development (UP-CMLD), and [§]Drug Discovery Institute, [⊥]Departments of Computational Biology and Structural Biology, University of Pittsburgh, Pittsburgh, Pennsylvania 15260, United States

Supporting Information

ABSTRACT: The interaction between small molecules and proteins is one of the major concerns for structure-based drug design because the principles of protein–ligand interactions and molecular recognition are not thoroughly understood. Fortunately, the analysis of protein–ligand complexes in the Protein Data Bank (PDB) enables unprecedented possibilities for new insights. Herein, we applied molecule-fragmentation algorithms to split the ligands extracted from PDB crystal structures into small fragments. Subsequently, we have developed a ligand fragment and residue preference mapping (LigFrag-RPM) algorithm to map the profiles of the interactions between these fragments and the 20 proteinogenic amino acid residues. A total of 4032 fragments were generated from 71 798 PDB ligands by a ring cleavage (RC) algorithm. Among these ligand fragments, 315 unique fragments were characterized with the corresponding fragment–residue interaction profiles by counting residues close to these fragments. The interaction profiles revealed that these fragments have specific preferences for certain types of residues. The applications of these interaction profiles were also explored and evaluated in case studies, showing great potential for the study of protein–ligand interactions and drug design. Our studies demonstrated that the fragment–residue interaction profiles generated from the PDB ligand fragments can be used to detect whether these fragments are in their favorable or unfavorable environments. The algorithm for a ligand fragment and residue preference mapping (LigFrag-RPM) developed here also has the potential to guide lead chemistry modifications as well as binding residues predictions.



BACKGROUND

The Protein Data Bank (PDB),¹ the largest protein structure database, is widely used in structure-based drug design. Several techniques have been developed for analyzing the interactions of protein–ligand complexes. For example, LIGPLOT² automatically analyzes and plots different intermolecular interactions, such as hydrogen bonds and ionic and aromatic interactions. Various sophisticated computer graphical interfaces, such as InsightII, Sybyl, and Maestro, are available for analyzing 3D structure of proteins and their complexes.

Large scale systematical analyses of the interactions between proteins and their ligands at the fragment level are rare. SuperStar³ and Relibase⁴ are two examples. These two computational tools analyze the interaction of functional groups between ligands and proteins and can superimpose these functional groups to create scatterplots of the specific interactions. Relibase is also a database search, retrieval, and analysis program for protein–ligand complex structures. Another similar tool is SIF (Structural Interaction Fingerprint),⁵ which generates 1D binary fingerprint representations of the intermolecular interactions in a 3D protein–inhibitor complex.

Recently, fragment-based approaches have been recognized as valuable tools in drug design. Dissecting a drug or small organic molecule into smaller fragment pieces and into even smaller discrete functional groups simplifies the computational analysis of ligand binding and identifies different pharmacophore elements required for high-affinity binding.⁶ The method is based on the principle that the proper optimization of each unique interaction in the binding site and subsequent incorporation into a single molecular entity should produce a compound with a binding affinity that is the sum of the individual interactions.⁶

Although successful applications of fragment-based approaches for drug discovery by NMR⁷ and X-ray crystallography⁸ have been reported earlier, these methods are quite time-consuming and expensive. Furthermore, the patterns of interactions between ligands and protein residues can be useful for the prediction of binding modes and structural adaptations.⁹ A statistical analysis of the binding sites of proteins would contribute greatly to the

Received: September 30, 2010

Published: March 18, 2011

understanding of the major determinants of ligand binding and specificity. Previous strategies or software tools have been limited in their ability to enumerate all of the fragments in PDB ligands and analyze the general interactions between the ligand fragments and protein residues.

We have therefore developed LigFrag-RPM, a novel ligand fragment and residue preference mapping algorithm. This approach splits the ligands in PDB complexes into fragments, analyzes the fragment–residue interactions, and subsequently derives the fragment–residue interaction profiles from multiple individual interactions. Developing the LigFrag-RPM algorithm offers a promising technique for the systematic benchmarking of protein–ligand interactions. The resulting profiles can be used to detect disfavored ligand fragments and develop a catalogue of preferred fragments for residues in the protein binding pockets as a tool to guide lead modification.

METHODS

Ligand Data Retrieval and Filtering. In order to explore and map the interactions between ligand fragments and protein residues, the following protocols were used to extract protein–ligand complexes after cleanup of ligand binding sites in the PDB.

First, Ligand Expo¹⁰ (<http://ligand-expo.rcsb.org/index.html>, accessed Dec 7, 2010) was used as the ligand resource in which ligands with their original coordinates were extracted from PDB crystal structure files. An advantage of the ligands compiled by Ligand Expo is that the PDB IDs are also encoded in the ligand names. Accordingly, the corresponding crystal structures can be readily identified. An example of a ligand name is ‘3gcs_BAX_1_A_401_B_’. In the Ligand Expo naming system, the first four characters, i.e. ‘3gcs’, represent the PDB ID, and BAX is the code for the cocrystallized ligand. A total of 456 642 ligand files were downloaded from Ligand Expo and were subjected to the subsequent filtering process, which removed ligands with less than six heavy atoms (such as solvents) and inorganic molecules (such as Mg^{2+} , Na^+ , and Mn^{2+}). Ligands without rings were also filtered out because the fragmentation algorithm requires at least one ring (see below). This filtering process was done by the SELECTOR module of Tripos Sybyl8.0. In addition, we also filtered out the PDB ligands files that contain either DNA or RNA by using the PDB advance search engine (<http://www.rcsb.org/pdb/search/advSearch.do>, accessed Dec 7, 2010). Finally, the PDB IDs were extracted from names of these qualified ligands. The corresponding PDB files were then downloaded from the PDB Web site. Only ligands from these complexes were considered in further analyses.

Using these criteria, a total of 71 798 ligands from 21 198 PDB complexes (as of Sep 28, 2009) passed the filters for further studies.

Ligand Fragmenting and Encoding. Ligands were split into small fragments to explore the individual interactions between these fragments and the 20 proteinogenic amino acid residues. We adopted the ring-cleavage fragmentation algorithm and the fragment encoding method established by Lameijer et al.¹¹ Molecules were split into ring systems, substituents, and various types of linkers, and these fragments were then encoded into strings containing the information of atoms, bonds, and connectivity. All of the unique fragment strings were then numbered by continuous integers starting with 0.

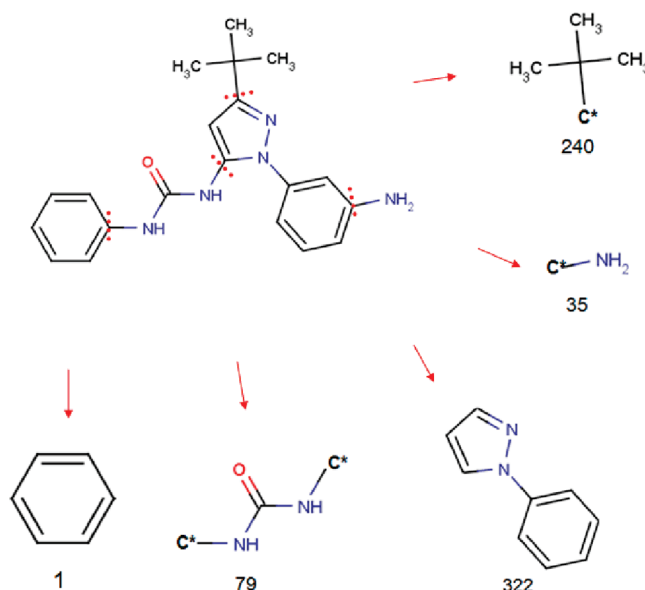


Figure 1. Ring cleavage (RC) algorithm for ligand fragmentation. This figure shows the ligand 1AW or 1-[1-(3-aminophenyl)-3-*tert*-butyl-1H-pyrazol-5-yl]-3-phenylurea and the fragments generated by the ring cleavage (RC) algorithm.

The algorithms used in our studies were developed with the open source software chemistry development kit (CDK),¹² and Marvin¹³ was used for displaying structures.

Generating Interaction Profiles. For each fragment, the corresponding interacting residues from protein–ligand complexes were recorded to generate the residue preference profile. An interacting residue of a fragment was originally defined as a residue containing at least one heavy atom located within 5 Å from any heavy atoms of the fragment. However, a threshold of 5 Å may include many residues that do not really interact with the fragment. We therefore restricted the threshold to require at least two heavy atoms of the residue to be located within less than 5 Å of the fragment’s heavy atoms. A residue close to a fragment was considered as an interacting residue, and was counted in the statistical analysis, only if it satisfied this criterion, which we named “2-pairs-in-5 Å”. The interactions of the ions and other small species with these ligand fragments are ignored, as we only analyze the interactions between ligand fragments and protein residues.

We assumed that if a fragment prefers one or more particular residues, the probability of these residues close to and interacting with this fragment should be higher than for those unfavorable residues in protein–ligand complexes. The occurrences of these 20 standard residues close to a fragment were counted as its interaction profile. However, many of these fragments may be overrepresented because of multiple occurrences in similar or even identical proteins in the PDB database. For example, querying with keywords “HIV-1 PROTEASE” retrieved 426 structures from the PDB database. Among them, 197 ligands were cocrystallized with HIV-1 protease. Especially, a ligand named 1UN or 2-[2-hydroxy-3-((3-hydroxy-2-methylbenzoyl)amino)-4-(phenylsulfanyl)butyl]decahydroisoquinoline-3-carboxylic acid *tert*-butylamide, occurs in 10 PDB structures with HIV-1 protease. Even though these PDB structures are in different resolutions or with different protein mutants, for most of the fragments of 1UN, the ligand environments or the nearby

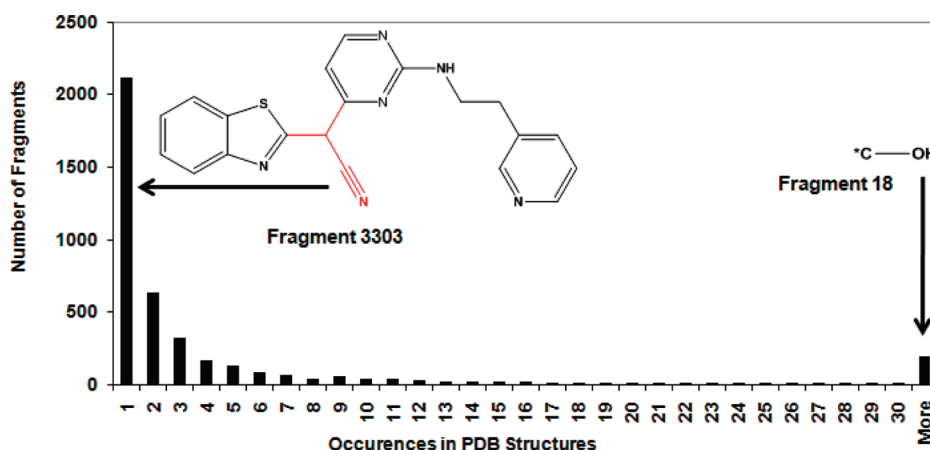


Figure 2. The histogram of the occurrences of 4032 ligand fragments from PDB structures. 2111 fragments occur only once in PDB structures (For example, fragment 3303 colored with red, occurs only in PDB 3CY3), 636 fragments occur twice, 319 fragments occur three times, and a total of 1346 fragments occur in at least four crystal structures (For example, fragment 18, or hydroxyl attached to carbon, occurs in 13 505 structures of our selected PDB complexes data set.).

residues are similar or identical. Considering the fragments from 1UN, the sum of the interactive residues would overrepresent the interacting residues in the binding pocket of HIV-1 protease. To remedy this problem, no-redundancy PDB (nr-PDB) IDs (<ftp://resources.rcsb.org/sequence/clusters/clusters70.txt>, accessed Dec 7, 2010) were used as a reference list to remove similar or identical proteins that interact with the same fragment. The nr-PDB IDs were compiled according to the sequence similarity of the proteins. Similar proteins were grouped into a cluster according to a similarity threshold of 70%. When multiple proteins from the same protein cluster interacted with the same fragment, we selected interacting residues only from a representative protein of this cluster. Because the focus of our study is about the interactions between residues and fragments, a protein with the highest number of interacting residues close to this fragment was selected as the representative protein. Other proteins in the same cluster with fewer interacting residues were discarded. An example of this selection process is described later.

After removal of redundant proteins for each individual fragment, all the interactive residues of a fragment were counted according to residue names. The original counts were then ranked in descending order. Note that the frequencies of 20 amino acids occurring in natural proteins are different, so normalization is necessary to calibrate these profiles. We took the residue frequencies from a published paper,¹⁴ which was calculated from 36 498 unique eukaryotic proteins.¹⁵ Each residue count in the original profile was then normalized by dividing with the correspondent residue frequency in all natural proteins.

RESULTS AND DISCUSSION

Fragmentation Results of PDB Ligands. Figure 1 is an illustration of the fragmentation result of the ligand 1AW or 1-[1-(3-aminophenyl)-3-*tert*-butyl-1*H*-pyrazol-5-yl]-3-phenylurea in PDB 3F3U. The ring-cleavage (RC) algorithm splits off the ring substituents (fragment 240 and fragment 35 in Figure 1), while the ring systems (fragment 322 and fragment 1) are intact. A linker (fragment 79) between fragment 322 and fragment 1 is also generated by the RC algorithm. Through this process, the ring cleavage algorithm yielded 4032 fragments

from these 71 798 PDB ligands, including 1404 rings, 1711 substituents, and 917 linkers.

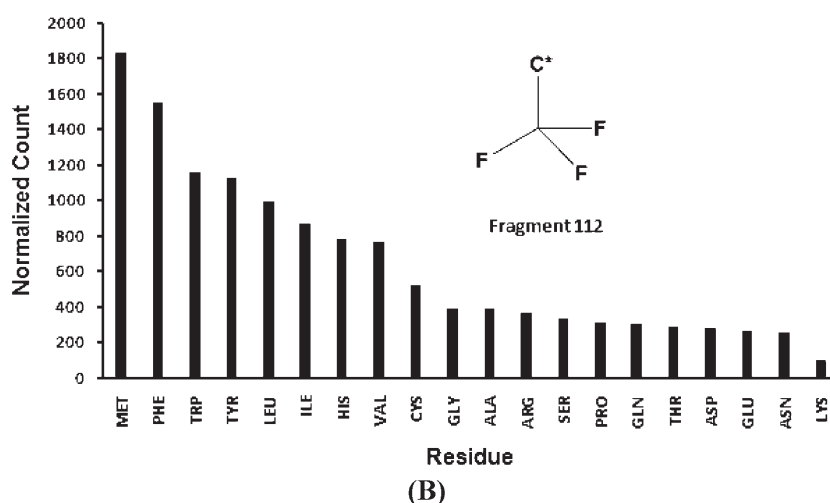
The frequencies of these fragments in PDB structures were analyzed next, as shown in Figure 2. Among the 4032 fragments, 2111 fragments appeared only once in the PDB structure files. For example, fragment 3003 (an acetone nitrile group) only appeared once in PDB 3CY3. In addition, 636 fragments appeared twice and 319 fragments appeared three times in PDB structures (Figure 2). These 3066 fragments (2111 + 636 + 319) were deleted and were not included in our studies. The remaining 1346 fragments appeared at least four times in crystal structures and were selected to generate the interaction profiles. The rationale was that the interaction profiles generated from fragments occurring in a limited number of cocrystal studies may be less meaningful.

Interaction Profiles of PDB Ligand Fragments. Fragment 112 (a trifluoromethyl group) serves as an example to illustrate how a fragment–residue interaction profile was generated (Figure 3A). The fragment 112 occurs in 238 cocrystallized ligands of 340 PDB complexes. According to the nonredundant PDB data (nr-PDB), the proteins in these 340 structures are from 77 clusters that were classified with 70% as the similarity threshold. For each cocrystal complex, the interactive residues of fragment 112 were identified by the 2-pairs-in-5 Å criterion. In each cluster, the protein that had the highest number of interacting residues with fragment 112 was selected as the representative protein for this cluster. A total of 77 representative proteins from these 77 clusters then were identified as a refined subset. All interactive residues of fragment 112 from the refined protein subset were counted according to residue names. As shown in Figure 3A, in ligand 3gcs_BAX_1_A_401_B (or the ligand BAX from PDB 3GCS), fragment 112 interacts with chain A of 3GCS (3GCS:A), which is in the cluster 3645 of the nr-PDB list. In this case, three ILEs (ILE84, ILE141, and ILE166), 1 HIS (HIS148), 1 LEU (LEU74), 1 MET (MET78), 1 VAL (VAL83), and 1 ASP (ASP168) were identified as interacting residues of fragment 112 (Figure 3A). While in the ligand 3gz9_D32_1_A_1_C (the ligand D32 from PDB 3GZ9), fragment 112 interacts with chain A of 3GZ9 (3GZ9:A), which is in the cluster 6994 of nr-PDB; 1 ILE (ILE249), 2 LEUs (LEU255 and LEU353), 2 VALs (VAL281 and VAL348), 1 ARG (ARG284), 1 PHE

Ligand name	Interactive residue counts					
	ILE	HIS	LEU	MET	TRP	...
3gcs_BAX_1_A_401_B__	3	1	1	1	0	...
3gz9_D32_1_A_1_C__	1	0	2	0	1	...
3bqm_BQM_1_B_1_C__	2	0	1	0	0	...
3e2m_E2M_1_B_1_C__	1	0	1	0	0	...
...

Original total residue counts	46	18	88	42	15	...
Frequency in natural proteins	0.053	0.023	0.089	0.023	0.013	...
Normalized total residue counts	867	782	988	1826	1153	...

(A)



(B)

Figure 3. An interaction profile is mapped out between fragment 112 and 20 amino acid residues. A: The interactive residues for fragment 112 (trifluoromethyl) in the nonredundant PDB structures are counted according to residues names, and the residue counts are then normalized by the correspondent residue frequencies in natural proteins. B: The graph plot of the interaction profile (normalized residues counts) for fragment 112. This interaction profile shows that the top five residues (MET, PHE, TRP, TYR, and LEU) are the most favored five residues whereas THR, ASP, GLU, ASN, and LYS are the least favored five residues for fragment 112.

(PHE352), and 1 TRP (TRP264) were identified as the interacting residues of fragment 112. If similar cocrystal complexes had limited interactive residues for a fragment, the interacting residues from those protein–ligand complexes were not considered in our analysis. For example, chain A of PDB 2ZNP (2ZNP:A) interacts with fragment 112 of the ligand K55 (2znp_K55_1_A_922_D__), and 2ZNP:A belongs to the same cluster (6994) of protein 3GZ9:A. However, fragment 112 in the protein 2ZNP:A has fewer interacting residues than 3GZ9:A. The interacting residues of fragment 112 from 2ZNP:A were therefore not counted, but interacting residues of fragment 112 from 3GZ9:A were considered when generating the fragment–residue interaction profiles.

An original (or non-normalized) interaction profile for fragment 112 was mapped by counting the interacting residues from these no-redundant proteins. The final interaction profile was then generated by normalizing the original profile with background residues frequencies, which demonstrates that fragment 112 prefers MET, PHE, TRP, TYR, and LEU most (Figure 3B). Moreover, the interaction profile not only revealed its main

preference for those five residues but also indicated its lowest preference to be LYS (Figure 3B), which is attributed to that fragment 112 favors more hydrophobic interaction with these residues than that with the polar residue LYS. An interesting observation is that TRP is located in a lower ranking position (15th) in the original profile, but it is located in a higher ranking position (3rd) after normalization. Such a normalization effect could be attributed to the fact that TRP appears more times near fragment 112 than it should according to its low occurrence in natural proteins.

The interaction profiles of other fragments were generated in the same way as for fragment 112. We ignored those interaction profiles where the maximum of their original residues counts are less than 10, because those profiles might have no statistical meaning. Only 315 interaction profiles remained after this filtration, and these corresponding 315 fragments were considered as the most popular fragments among the PDB ligands, including methoxy, benzene, piperidine, pyridine, etc. The 315 fragments and their original fragment–residue interaction profiles together with the normalized profiles are listed in Part 1 and Part 2 of the Supporting Information, respectively.

Residue Preference of PDB Ligand Fragments. The ranking positions of the original residue-count profiles reflect the residue preference in the protein binding pockets. By analyzing the 315 original (non-normalized) interaction profiles, LEU appears more often nearby most of these 315 popular fragments. Figure 4 shows that LEU occurred in the first ranking position in 89 of the 315 original profiles, and LEU never occurs at lowest ranking position in any of the 315 original profiles. This result is congruent with the publication that LEU is the most popular residue among the protein amino acids,¹⁶ and that the probability of its occurrence near the binding pocket is much higher than for any other residues. LEU, as a nonpolar hydrophobic residue, has the proper size, is not too bulky compared to TRP, is not too small compared to ALA, and has a flexible side chain that can exhibit London dispersion interactions and adapt to a broad range of ligands. Therefore, LEU is suitable to interact with benzene, naphthalene, indole, F, Cl, Br, and NO₂ fragments. In contrast,

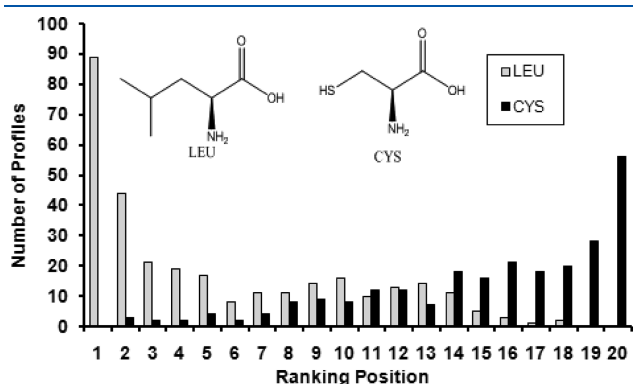


Figure 4. The histogram of ranking positions of LEU and CYS in the 315 original (non-normalized) fragment–residue interaction profiles. The histogram shows that LEU is found in the first ranking position in 89 of the 315 original interaction profiles, but it is not found in the 19th or 20th ranking positions of any original profiles. The histogram also shows that CYS is found in the 20th ranking position in 56 of the 315 original interaction profiles but it is not found in the first ranking position in any original profile.

the CYS residue was found more often at the lower positions for most of these 315 original profiles. It appeared in the 20th ranking position in 56 original profiles, while it did not appear in the first ranking position in any of these 315 original profiles (Figure 4).

To further analyze the residues preference for each fragment, we defined the count ratio of a profile as the ratio of the highest residue count divided by the lowest residue count in the normalized profiles. A high count ratio usually means that this fragment has a high preference for certain types of residues. If a residue count in a non-normalized profile is zero, a corrected profile is generated by adding 0.5 as a pseudocount to all the original residues counts in this profile to avoid division by zero. Such corrections were also made in other cheminformatics tools such as Molprint2D software.¹⁷ The corresponding count ratio was calculated based on the normalized corrected profile. A histogram (Figure 5) was generated from these 315 count ratios, showing that the count ratios range from 2.62 to 239.62 with a mean value of 36.78. Among these 315 fragment–residue interaction profiles, 262 profiles had count ratios larger than 10, and 197 profiles had count ratios larger than 20. Obviously, the data indicate that most of the 315 fragments had specific preferences for certain types of residues.

Potential Application of the Interaction Profiles by Case Studies. We have shown how our LigFrag-RPM algorithm was used to generate the profiles of fragment–residue interactions. We further demonstrated in the studies shown below that these profiles can be used to guide the structure-based design or chemistry optimization of a lead compound by analyzing the residues close to each individual fragment of the lead based on the generated interaction profiles. Two examples of such studies are illustrated here and more are given in Part 3 of the Supporting Information.

The serine protease factor Xa has a unique role in the coagulation cascade and represents an interesting target for the development of novel anticoagulants. Zbinden et al.¹⁸ reported the identification of novel 3-aminopyrrolidine factor Xa inhibitors and their cocrystallized structures in 2009. The reported inhibitor LZI was cocrystallized with factor Xa in PDB 2VWM. In our study, this ligand was fragmentized by the ring-cleavage algorithm and then the interacting residues of individual

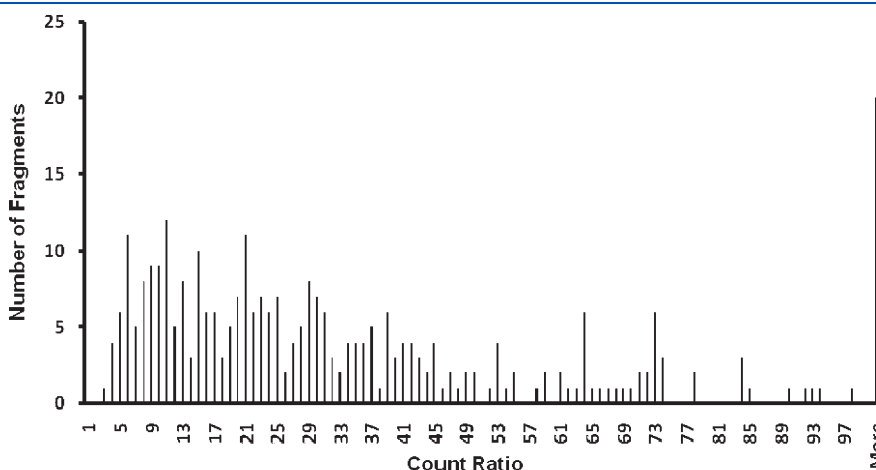


Figure 5. The histogram for count ratios of 315 fragment–residues interaction profiles generated from popular fragments. The histogram shows that the count ratios of these 315 interaction profiles are in a range of a minimum of 2.62 to a maximum of 239.62 and a mean value of 36.78. 262 of these 315 profiles have the count ratios larger than 10 and 197 of these 315 profiles have the count ratios larger than 20. The count ratio represents the residues preference for each fragment and is defined as the ratio of the highest residue count divided by the lowest residue count in the normalized profile.

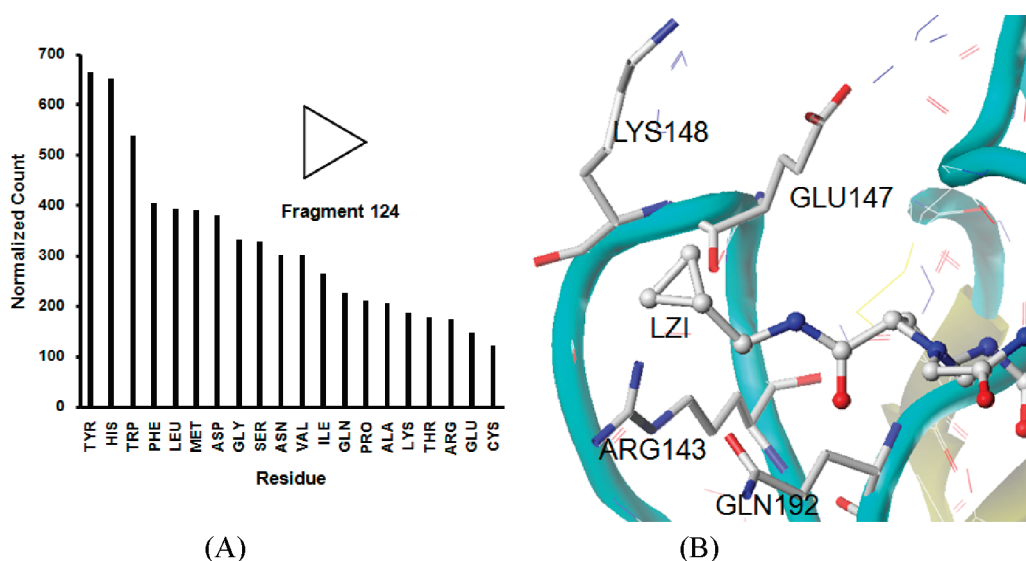


Figure 6. The fragment–residue interaction profile of fragment 124 (A) and the surrounding residues of fragment 124 in the crystal structure of PDB 2VWM (B). Fragment 124 (cyclopropane) is surrounded by ARG143, GLU147, LYS148, and GLN192 of factor Xa in PDB 2VWM. These four residues are located at the lower ranking positions of the interaction profile of fragment 124, 18th, 19th, 16th, and 13th, respectively. It is therefore not in its most favorable environment according to its fragment–residue interaction profile.

fragments were identified by the 2-pairs-in-5 Å criterion. Among the generated fragments, fragment 124 (cyclopropane) is surrounded by ARG143, GLU147, LYS148, and GLN192 (Figure 6B). However, these four residues are located at the lower ranking positions of the interaction profile of fragment 124 (Figure 6A), 18th, 19th, 16th, and 13th, respectively. Such low ranking positions calculated by our program indicate that fragment 124 is not in its favorite environment and also suggest that fragment 124 may not be a required functional group for factor Xa inhibition. In our further study, we found that another ligand (H22 in PDB 2VVU) without fragment 124 still shows a 10-fold higher affinity ($K_i = 8$ nM) than LZI ($K_i = 93$ nM). This result confirmed our prediction and is consistent with our analysis of the derived fragment–residue interaction profile.

Furthermore, we have explored the established LigFrag-RMP method in the study of the selectivity of a compound for guiding the lead chemistry optimization by analyzing the fragment–residue interaction profiles of this compound. As illustrated in Figure 7, ovalicin is an inhibitor of methionine amino peptidases, and the structures of human type 1 and type 2 methionine aminopeptidases (MetAP1 and MetAP2) in complex with ovalicin were reported as PDB 2GZ5¹⁹ and PDB 1B59,²⁰ respectively. It is known that ovalicin binds with lower affinity to MetAP1 than to MetAP2. In 2GZ5, the methoxy group (fragment 0) is surrounded by HIS303, HIS310, and CYS301 (Figure 7B), whereas HIS is in the 5th and CYS is in the 10th ranking position of the interaction profile of fragment 0. In 1B59, the methoxy group is surrounded by ASN329, GLY330, HIS331, and HIS339 (Figure 7C), whereas ASN, GLY, and HIS are in the 7th, 12th, and 5th ranking positions, respectively. As shown in Figure 7C, GLY is not a favorite residue of fragment 0 whereas ASN in MetAP2 (1B59) is more preferred by fragment 0 than CYS in MetAP1 (2GZ5). In addition, the residue ASN has water-bridged interaction with an OH group in the sugar ring of ovalicin (not shown in Figure 7C). The methoxy group, therefore, is in a more preferred environment in MetAP2 than in MetAP1. This observation can partly explain the binding affinity difference between the inhibitor and the two target proteins.

In contrast, it should also be possible to modify this ligand in PDB 2GZ5 by substituting fragment 0 (methoxy group) with other fragments that are preferred by HIS or CYS residues. The question then is which fragments should be chosen to pursue the lead optimization chemistry? By analyzing the profiles of the 315 most popular fragments identified above, a few fragments that have HIS in the top ranking positions of their profiles are easily found. Table 1 summarizes the structures of six identified putative fragments that have favored interactions with HIS, and the corresponding interactive profiles of these fragments. Accordingly, we believe that the established algorithm can be used as an alternative strategy to select the optimal fragment or substituent for the lead chemistry modification. Of course, other factors such as fragment size and orientation should also be considered carefully when replacing a fragment. It also should be mentioned that as the positioning of a new fragment can be influenced by where and how its predecessors are placed, this kind of fragment replacement may not always be successful. However, our studies did provide options of introducing various fragments for lead modification of an active molecule in order to enhance the bioactivity.

Limitations of the LigFrag-RPM. Our LigFrag-RPM method analyzed the residues close to a fragment and generated the fragment–residue interaction profile. However, the current version of the program also has some limitations that will need further improvements. For example, LigFrag-RPM still requires users to manually analyze the relevant interactions, such as covalent bonds, hydrogen-bond interactions, charge–charge interactions, or hydrophobic interactions. An extreme case is that the profile of fragment 23 (Figure 8) has ASN (original count is 1632, and the normalized count is 37 953) as its most favored residue, followed by TYR (original count is 457, and the normalized count is 21 000), and ALA as the least favored residue (original count is 187, and the normalized count is 2561), as shown in Figure 8. The count ratio for the fragment is 14.82 (i.e., $37\,953/2561 = 14.82$). The result reveals that fragment 23 may

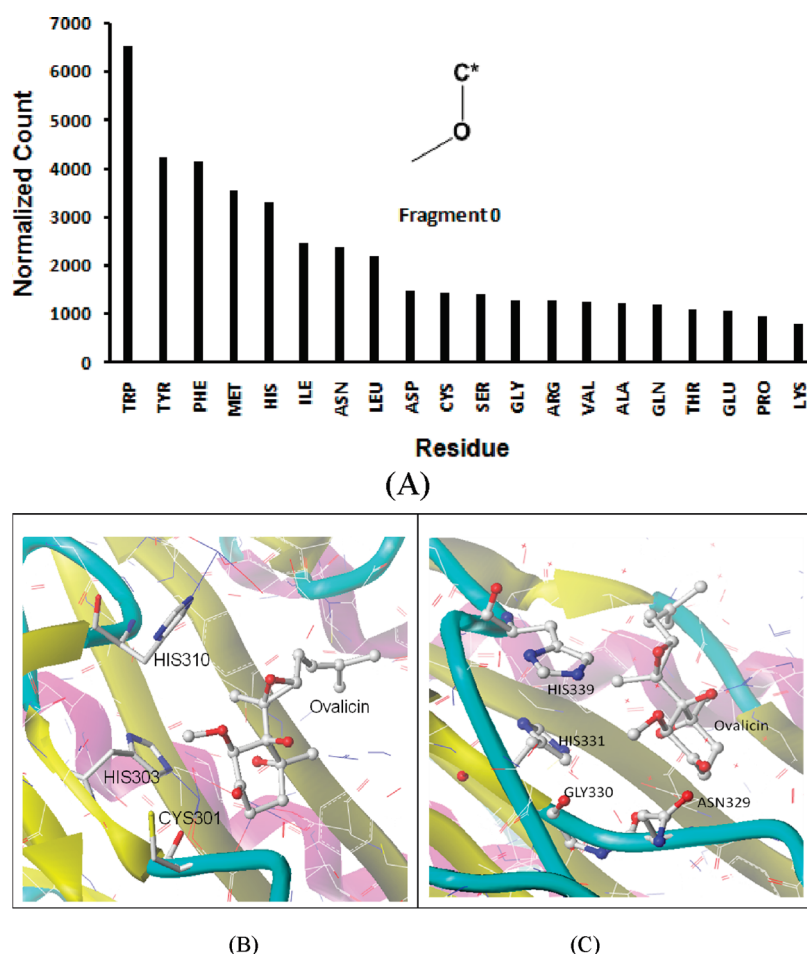


Figure 7. The fragment–residue interaction profile of fragment 0 (methoxy group) (A) and the surrounding residues of fragment 0 in the crystal structures of PDB 2GZS (B) and PDB 1B59 (C). The structure of PDB 2GZS (B) shows the interactions between ovalicin and human type 1 methionine aminopeptidase, and the methoxy group (fragment 0) is surrounded by HIS303, HIS310, and CYS301 where HIS is in the 5th ranking position and CYS is in the 10th ranking position of its interaction profile. The structure of PDB 1B59 (C) shows the interactions between ovalicin and human type 2 methionine aminopeptidase, and the methoxy (fragment 0) is surrounded by HIS339, HIS331, GLY330, and ASN329 where ASN, GLY, and HIS are in the 7th, 12th, and 5th ranking positions of its interaction profile, respectively.

have specific interactions with the residue ASN. Actually, one approved drug molecule deposited in DrugBank,²¹ *N*-acetyl-D-glucosamine (NAG, DrugBank ID DB00141), has exactly this fragment. NAG is cocrystallized with its target protein SPP-40 (PDB ID 1XH9, Figure 8). The N atom of fragment 23 is 3.01 Å apart from the N atom of the amide of ASN39, because the C1 atom in the NAG ring is covalently bound to the N atom of amide in ASN39 (the distance is 1.42 Å). Thus, caution is needed when analyzing the residue preferences by the interaction profiles because the adjacent fragments often influence each other.

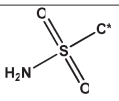
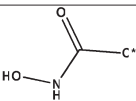
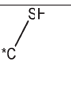
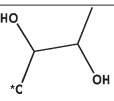
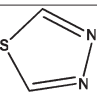
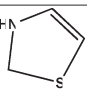
In addition, the interactions can occur between residues and a molecular fragment composed of part of a ring+nonring. Although we counted the residues that interact with two or more fragments simultaneously, other fragmentation algorithms should be considered for the analysis of the interaction between residues and ring+no-ring fragments. Note that crystallization conditions can also influence the interaction between the fragments and the residues, but such information cannot be easily incorporated in our statistical analysis. For example, amino acid charges could be different and interactions involved would change significantly upon various pH conditions for crystallization. Fortunately, a study conducted by Kantardjieff and Rupp²² reported that “the frequency

distribution for the reported crystallization pH of proteins is unimodal, with mean = 6.7, median = 6.9”. Their results show that most of the reported proteins were crystallized at nearly neutral (or physiological) pH values. However, caution about pH influence still needs to be taken when using these profiles for individual structure analysis. Compared to traditional energy-based protein–ligand interaction analysis, the interaction profiles generated by LigFrag-RPM with statistical methods are only qualitative and can be an alternative for data-mining protein–ligand interactions. It is obvious that not all profiles of the fragments in a known binding affinity complex can be acquired because some of these fragments are very rare in PDB structures. It thus is challenging to quantitatively link the contribution of each residue–fragment to the binding free energy for the current approach. However, as one can see from the case studies, the interaction profile directly links the fragment and its preferred residues. It therefore can be used as an alternative data-mining tool to guide fragment-based drug design.

CONCLUSIONS

We have presented a novel algorithm, LigFrag-RPM, for fragment–residue interaction analysis and also validated it through the

Table 1. Interaction Profiles of Six Fragments with HIS in the Top Ranking Positions

Fragment ID	135	180	246	260	369	402
Structure						
	HIS 1434 TRP 923 THR 321 VAL 301 SER 219 MET 217 PHE 214 LEU 146 LYS 125 ASN 116 ARG 115 GLY 97 ASP 80 PRO 76 GLN 75 TYR 60 ILE 56 GLU 49 ALA 41	HIS 1173 TRP 153 TYR 151 PRO 134 GLY 125 GLU 98 ARG 96 ASP 80 PHE 71 ALA 54 GLN 50 MET 43 CYS 40 LEU 22 ILE 18 SER 13	HIS 2913 ARG 903 GLY 513 TRP 2692 CYS 1000 GLN 625 PHE 571 SER 273 GLU 311 TYR 545 ALA 219 ASP 280 MET 521 LEU 123 ASN 232 VAL 142 ILE 113 LYS 93 THR 107 PRO 96	TRP 846 HIS 521 TYR 272 PHE 238 GLN 150 GLU 131 MET 130 ILE 113 LEU 112 SER 109 ASP 80 CYS 80 VAL 79 ALA 68 PRO 38 THR 35 GLY 27 ASN 23 ARG 19	HIS 478 THR 214 GLN 125 VAL 111 LEU 78 TRP 76 ALA 41 GLU 32 TYR 30 PHE 23 ASP 20 GLY 13	HIS 304 MET 217 TYR 151 LEU 134 ILE 113 GLY 97 VAL 79 TRP 76 ASP 60 ALA 41 CYS 40 LYS 31 SER 27 PHE 23 THR 17 GLU 16

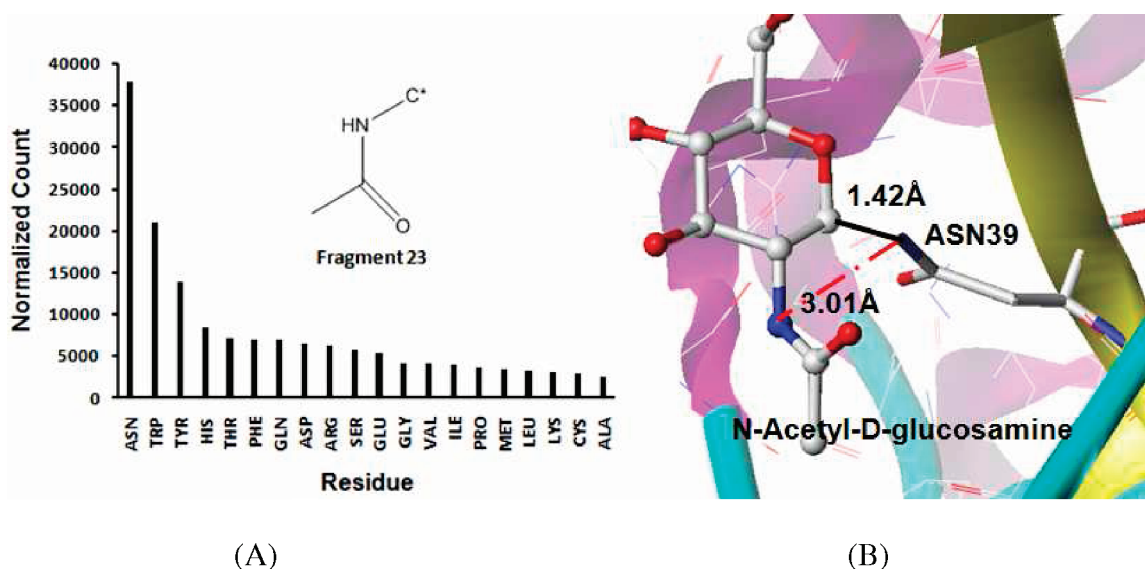


Figure 8. The fragment–residues interaction profiles of fragment 23 (A) and fragment 23 in *N*-acetyl-D-glucosamine from PDB 1XHG (B). A: The interaction profiles demonstrated that ASN is the most favorable residue and CYS is the least favorable residue for fragment 23. B: In PDB 1XHG, *N*-acetyl-D-glucosamine is cocrystallized with its target protein SPP-40. The N atom of fragment 23 is 3.01 Å from the N atom of amide of ASN39 because the C1 of NAG ring is covalently bound to the N atom of the amide in ASN39 (The distance is 1.42 Å).

illustrated case studies. This algorithm fragmentizes the ligands in the PDB and then counts the interactive residues to generate the fragment–residue interaction profiles. Our results indicate that most fragments have specific preferences for certain types of residues. We also demonstrated that the interaction profiles

generated by the LigFrag-RPM algorithm can be used to identify whether a molecular fragment or functional group is in its favored or a rather unfavorable environment, and potentially to guide lead modification by replacing the residue-mismatched fragment with other more residue-matched fragments. The profile of each

fragment derived from multiple protein–ligand complexes can help to estimate the probability of each amino acid residue around a fragment and thus may also be used potentially to guide site-directed mutagenesis studies of the protein binding pocket.

The current LigFrag-RPM algorithm is still at an evolutionary stage. The fragments from which we generated the LigFrag-RPM profiles represent only a small number of all possible fragments. For example, Lameijer et al.¹¹ reported their studies of the fragmentation of 250 251 compounds in the NCI library using a ring-cleavage algorithm yielding 65 612 fragments, which represents a much larger collection than those from the PDB. With increasingly available protein–ligand complexes in PDB, the diversity and number of fragments will help us to refine our algorithm. Furthermore, we are also exploring another potential application to use the developed profiles as a primary filtering process in our docking and virtual screening studies to remove ineligible compounds of a target protein, which will be reported elsewhere.

■ ASSOCIATED CONTENT

Supporting Information. The structures of the 315 fragments are given in Part 1. The fragment–residue interaction profiles of these 315 fragments are listed in Part 2. Part 3 provides four additional examples of PDB fragment–residue interaction analysis. This material is available free of charge via the Internet at <http://pubs.acs.org>.

■ AUTHOR INFORMATION

Corresponding Author

*Tel.: +1-412-383-5276; fax: +1-412-383-7436; e-mail: xix15@pitt.edu

■ ACKNOWLEDGMENT

We acknowledge Dr. Lei Wang and Dr. Tom Jones at Tripos Company for technical support. We would like to thank Dr. Herbert Barry III for reading the manuscript. This project is supported by grants from NIH (NIGMS P50-GM067082 and R01 DA025612).

■ REFERENCES

- (1) Berman, H. M.; Westbrook, J.; Feng, Z.; Gilliland, G.; Bhat, T. N.; Weissig, H.; Shindyalov, I. N.; Bourne, P. E. The Protein Data Bank. *Nucleic Acids Res.* **2000**, *28* (1), 235–42.
- (2) Wallace, A. C.; Laskowski, R. A.; Thornton, J. M. LIGPLOT: a program to generate schematic diagrams of protein–ligand interactions. *Protein Eng.* **1995**, *8* (2), 127–34.
- (3) Verdonk, M. L.; Cole, J. C.; Taylor, R. SuperStar: a knowledge-based approach for identifying interaction sites in proteins. *J. Mol. Biol.* **1999**, *289* (4), 1093–108.
- (4) Hendlich, M.; Bergner, A.; Gunther, J.; Klebe, G. Relibase: design and development of a database for comprehensive analysis of protein–ligand interactions. *J. Mol. Biol.* **2003**, *326* (2), 607–20.
- (5) Deng, Z.; Chuaqui, C.; Singh, J. Structural interaction fingerprint (SIFt): a novel method for analyzing three-dimensional protein–ligand binding interactions. *J. Med. Chem.* **2004**, *47* (2), 337–44.
- (6) Hajduk, P. J.; Greer, J. A decade of fragment-based drug design: strategic advances and lessons learned. *Nat. Rev. Drug Discovery* **2007**, *6* (3), 211–9.
- (7) Shuker, S. B.; Hajduk, P. J.; Meadows, R. P.; Fesik, S. W. Discovering high-affinity ligands for proteins: SAR by NMR. *Science* **1996**, *274* (5292), 1531–4.

- (8) Nienaber, V. L.; Richardson, P. L.; Klighofer, V.; Bouska, J. J.; Giranda, V. L.; Greer, J. Discovering novel ligands for macromolecules using X-ray crystallographic screening. *Nat. Biotechnol.* **2000**, *18* (10), 1105–8.
- (9) Gunther, J.; Bergner, A.; Hendlich, M.; Klebe, G. Utilising structural knowledge in drug design strategies: applications using Relibase. *J. Mol. Biol.* **2003**, *326* (2), 621–36.
- (10) Feng, Z.; Chen, L.; Maddula, H.; Akcan, O.; Oughtred, R.; Berman, H. M.; Westbrook, J. Ligand Depot: a data warehouse for ligands bound to macromolecules. *Bioinformatics* **2004**, *20* (13), 2153–5.
- (11) Lameijer, E. W.; Kok, J. N.; Back, T.; Ijzerman, A. P. Mining a chemical database for fragment co-occurrence: discovery of “chemical clichés” *J. Chem. Inf. Model* **2006**, *46* (2), 553–62.
- (12) (a) Steinbeck, C.; Han, Y.; Kuhn, S.; Horlacher, O.; Luttmann, E.; Willighagen, E. The Chemistry Development Kit (CDK): an open-source Java library for Chemo- and Bioinformatics. *J. Chem. Inf. Comput. Sci.* **2003**, *43* (2), 493–500. (b) Steinbeck, C.; Hoppe, C.; Kuhn, S.; Floris, M.; Guha, R.; Willighagen, E. L. Recent developments of the chemistry development kit (CDK) - an open-source java library for chemo- and bioinformatics. *Curr. Pharm. Des.* **2006**, *12* (17), 2111–20.
- (13) Marvin5.0.2.1, ChemAxon (<http://www.chemaxon.com>, accessed Dec 7, 2010).
- (14) Halabi, N.; Rivoire, O.; Leibler, S.; Ranganathan, R. Protein sectors: evolutionary units of three-dimensional structure. *Cell* **2009**, *138* (4), 774–786.
- (15) Lockless, S. W.; Ranganathan, R. Evolutionarily conserved pathways of energetic connectivity in protein families. *Science* **1999**, *286* (5438), 295.
- (16) Carlson, H. A.; Smith, R. D.; Khazanov, N. A.; Kirchhoff, P. D.; Dunbar, J. B., Jr.; Benson, M. L. Differences between high- and low-affinity complexes of enzymes and nonenzymes. *J. Med. Chem.* **2008**, *51* (20), 6432.
- (17) Bender, A.; Mussa, H. Y.; Glen, R. C.; Reiling, S. Molecular similarity searching using atom environments, information-based feature selection, and a naive bayesian classifier. *J. Chem. Inf. Comput. Sci.* **2004**, *44* (1), 170–178.
- (18) Zbinden, K. G.; Anselm, L.; Banner, D. W.; Benz, J.; Blasco, F.; Decoret, G.; Himber, J.; Kuhn, B.; Panday, N.; Ricklin, F.; Risch, P.; Schlatter, D.; Stahl, M.; Thomi, S.; Unger, R.; Haap, W. Design of novel aminopyrrolidine factor Xa inhibitors from a screening hit. *Eur. J. Med. Chem.* **2009**, *44* (7), 2787–95.
- (19) Addlagatta, A.; Matthews, B. W. Structure of the angiogenesis inhibitor ovalicin bound to its noncognate target, human Type 1 methionine aminopeptidase. *Protein Sci.* **2006**, *15* (8), 1842–8.
- (20) Liu, S.; Widom, J.; Kemp, C. W.; Crews, C. M.; Clardy, J. Structure of human methionine aminopeptidase-2 complexed with fumagillin. *Science* **1998**, *282* (5392), 1324.
- (21) (a) Wishart, D. S.; Knox, C.; Guo, A. C.; Cheng, D.; Shrivastava, S.; Tzur, D.; Gautam, B.; Hassanali, M. DrugBank: a knowledgebase for drugs, drug actions and drug targets. *Nucleic Acids Res.* **2008**, *36* (Database issue), D901–6. (b) Wishart, D. S.; Knox, C.; Guo, A. C.; Shrivastava, S.; Hassanali, M.; Stothard, P.; Chang, Z.; Woolsey, J. DrugBank: a comprehensive resource for in silico drug discovery and exploration. *Nucleic Acids Res.* **2006**, *34* (Database issue), D668–72.
- (22) Kantardjieff, K. A.; Rupp, B. Protein isoelectric point as a predictor for increased crystallization screening efficiency. *Bioinformatics* **2004**, *20* (14), 2162.